THE ASTROPHYSICAL JOURNAL, 276:761–765, 1984 January 15

A STUDY OF THE EVOLUTION OF ENERGETIC ELECTRONS IN A SOLAR FLARE

GORDON D. HOLMAN AND M. R. KUNDU
Astronomy Program, University of Maryland

AND

B. R. DENNIS
Laboratory for Astronomy and Solar Physics, NASA Goddard Space Flight Center
Received 1983 March 28; accepted 1983 June 17

ABSTRACT

The impulsive microwave and hard X-ray emissions from the 1980 June 25 (1550 UT) solar flare are studied. Time profiles are obtained for the four major bipolar regions that were found by Kundu, Schmahl, and Velusamy to contribute to the 6 cm emission from the flare. The light curves are found to be consistent with the regions flaring in unison (to within the 10 s time resolution of the VLA observations) rather than sequentially or in an uncorrelated manner. There is no indication of any change in the magnetic field structure in the emitting regions to within the 2″ spatial resolution of the observations.

The maximum 6 cm microwave flux occurs 1.4 minutes after the maximum in the integrated 28–498 keV X-ray emission and coincides with a secondary peak in the X-ray light curve. This is explained by the observation that the X-ray spectrum, and, hence, the electron spectrum, is harder at the time of the 6 cm flux maximum. The results show a clear correlation between the X-ray flux greater than 100 keV and the microwave flux. The power flux of electrons with energy greater than 25 keV (assuming thick-target bremsstrahlung for the X-ray emission) does not increase at the time of the 6 cm flux maximum, however, even though the largest number of electrons with energy greater than 100 keV is produced at this time. The implications of this result are discussed. The steep, low-frequency microwave spectrum at the time of the 6 cm maximum indicates that the emission at this time is nonthermal. The spectral behavior of the hard X-ray emission is found not to be consistent with the betatron acceleration mechanism.

Subject headings: particle acceleration — radiation mechanisms — Sun: flares — Sun: radio radiation — Sun: X-rays

I. INTRODUCTION

One of the major goals of solar flare research is to determine the origin and evolution of energetic electrons accelerated during the impulsive phase of a flare. These particles are most directly observable through their gyrosynchrotron radiation at microwave frequencies and their emission of hard X-rays through collisional bremsstrahlung. While the microwave and hard X-ray emissions both depend upon the distribution of energetic electrons in the flaring region, they also depend upon the magnetic field and thermal plasma distributions in the region. The magnetic field strength and direction delimit the regions where the microwave emission is most intense. The hard X-ray emission is greatest in regions where the plasma density is high. Hence, for studying the acceleration and propagation of energetic electrons during a flare, simultaneous observations at microwave and hard X-ray frequencies are most fruitful.

A major flare for which high quality microwave and hard X-ray data are available occurred on 1980 June 25 at 1550 UT. Flare maps at 6 cm wavelength with arc second spatial resolution and 10 s time resolution were obtained with the Very Large Array (VLA) (Kundu, Schmahl, and Velusamy 1982; hereafter KSV). Microwave spectral data (total intensity, no spatial resolution) from Sagamore Hill and Bern are also available. X-ray spectra (28–498 keV) were obtained with the hard X-ray burst spectrometer (HXRBS) aboard the *Solar Maximum Mission* satellite (*SMM*). The HXRBS instrument is described by Orwig, Frost, and Dennis (1980). The VLA observations and results (as well as Hα data and some aspects of the Sagamore Hill and HXRBS data) have been described by KSV. In this paper we use the combined microwave and hard X-ray data to study the evolution of energetic electrons accelerated during the impulsive phase of the June 25 flare.

II. ANALYSIS OF THE 6 CENTIMETER VLA MAPS

An interesting aspect of the 6 cm VLA maps for the June 25 flare is that they show a complex, multiple source structure. KSV identify eight individual sources which contribute to the total 6 cm emission throughout the period of the flare. Four of these sources are aligned along an approximately E–W line and persist throughout most of the flare. From the most eastern source to the western source they are labeled B-A-D-C by KSV. The 6 cm emission is dominated by source A throughout most of the flare. The maps show each of these sources to be elongated, bipolar structures, indicating that they are individual arcades of magnetic loops (see KSV).

We have used the cleaned VLA maps to produce light curves for the flare sources, so that the evolution of each source can be studied individually. A similar, less quantitative study was made by KSV, but these authors used 1 minute time averages of the 10 s maps for their analysis. Here we use the 54 10 s maps obtained during the impulsive phase of the flare (1551–1600 UT). Relative source intensities were

determined for each 10 s time frame by integrating the positional fluxes within a fixed rectangular box centered upon the source. The box size was determined by the need to include the entire source while avoiding contamination from adjacent sources throughout the entire flare sequence. Light curves for the four major bipolar regions A–D are shown in Figure 1. The light curves for sources B, A, and D are seen to be similar, with a peak near $15^h53^m.4$ UT (the time at which the total 6 cm emission is maximum) and a broad peak before 15^h52^m UT. The emission from source C is seen to plunge to a minimum when the emission from the other regions is greatest. Source C is the weakest of the four, however, and this most likely reflects the limited dynamic range of the VLA observations rather than a true dimming of the source.

Our light curves do not reflect the more random variations indicated in Table 1 of KSV. We find the source variations to be more highly correlated than their table indicates. This can be attributed primarily to their use of integrated, 1 minute maps. Our results are consistent with sources B, A, and D, and probably all four sources, varying in unison.

The separation between sources B and C is $\sim 40''$, or 17,000 km. For simultaneous variations within the instrumental resolution of 10 s, a signal speed of 1700 km s^{-1} or greater is required. For a magnetic field strength of 100 gauss and a plasma density of 10^{10} cm^{-3}, the Alfvén speed is 2800 km s^{-1}. Hence, the simultaneous (to within 10 s) variation of sources with this separation is not unreasonable. We cannot rule out the possibility that some of the sources are not real, but are artifacts of the mapping procedure. This possibility does not seem likely, however, given the persistence of the sources throughout the flare. It is interesting to note that, down to the instrumental resolution of $\sim 1''$, the 6 cm maps do not show any significant change in the magnetic field structure throughout the period of the flare (other than a uniform shift in position, discussed by KSV).

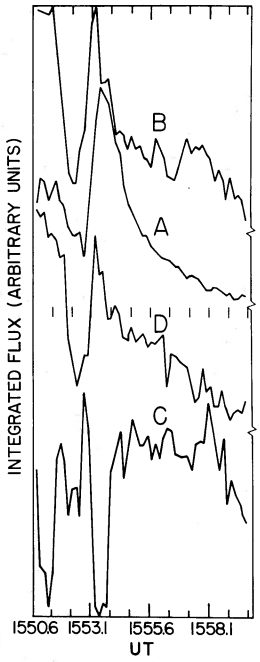

FIG. 1.—Light curves are shown for the four major 6 cm sources which appear in the VLA maps. The flux scale is linear, and the difference between the maximum and the minimum flux is normalized to the same value for each source.

III. ANALYSIS OF THE HARD X-RAY AND MICROWAVE SPECTRAL DATA

HXRBS X-ray light curves in the energy bands 28–56, 56–129, asd 104–498 keV are shown in Figure 2. Sagamore Hill microwave data at 2.7 GHz (11 cm), 5 GHz (6 cm), 8.8 GHz (3.4 cm), and 15.4 GHz (2 cm) are shown in Figure 3. As was noted by KSV, the integrated (≥ 28 keV) hard X-ray flux reaches its highest value at 15^h52^m UT, whereas the 6 cm flux reaches its highest value at $15^h53^m.4$ UT. They suggest that this may be due either to the lack of sensitivity of the VLA to extended structures, or to

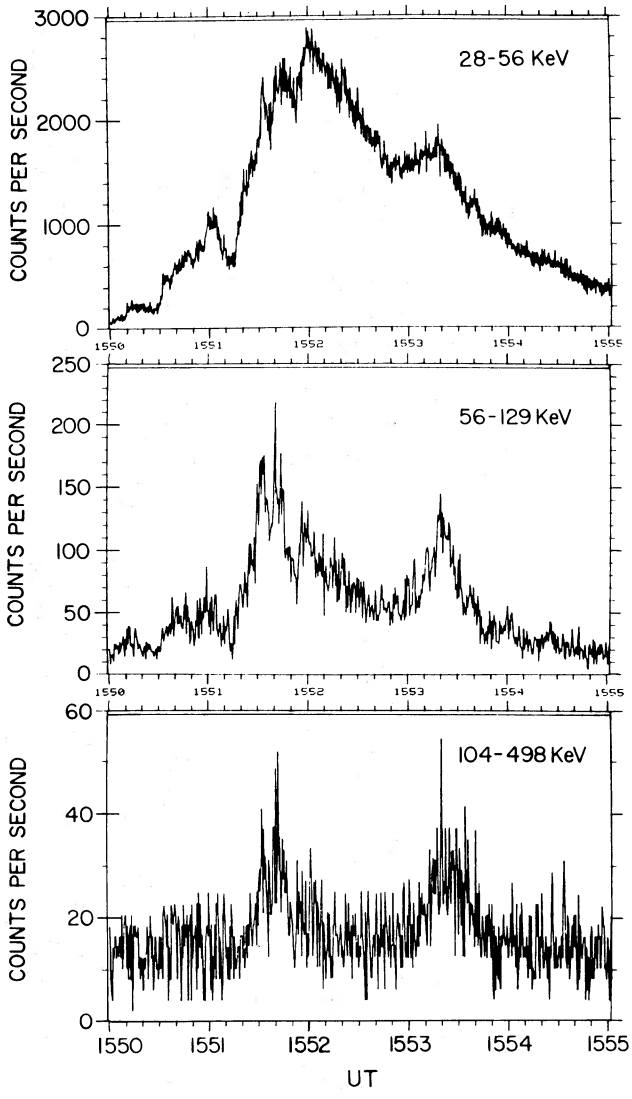

FIG. 2.—HXRBS X-ray light curves are shown in three energy bands for the impulsive phase of the flare. The sample average (time resolution) is 0.256 s in the lowest energy band, and 0.512 s in the two highest energy bands.

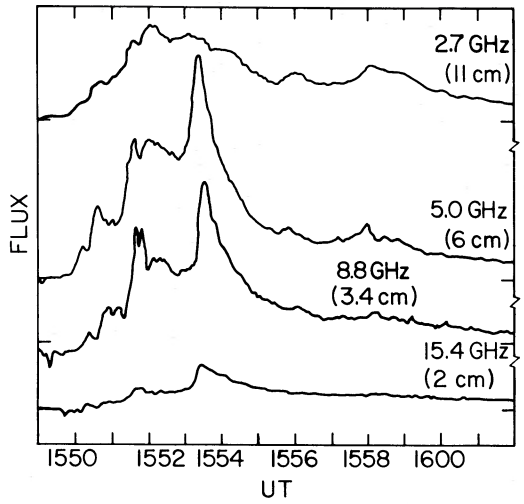

FIG. 3.—Sagamore Hill light curves at four microwave frequencies are shown. The flux scale is linear, and the peak flux and each frequency is 80 sfu (2.7 GHz), 294 sfu (5.0 GHz), 269 sfu (8.8 GHz), and 111 sfu (15.4 GHz) (1 sfu = 10^{-22} W m^{-2} Hz^{-1}).

the observation of regions by the VLA which emit most of their X-rays at energies below 28 keV. The first possibility is ruled out by the 6 cm Sagamore Hill light curve, which also reaches its highest value at $15^h53^m.4$ UT (the single-dish Sagamore Hill observation is sensitive to extended structures, since it integrates emission from the whole Sun). The time profiles in Figure 2 indicate that the second possibility is also incorrect: although the lowest energy X-ray emission is maximum at 1552 UT, the higher energy X-rays ($\gtrsim 50$ keV) show peak emission at $15^h51^m42^s$ UT and $15^h53^m20^s$ UT. The peak at 1553 UT becomes more prominent for higher energy X-rays. Hence, we conclude that the maximum 6 cm radio emission occurs after the integrated hard X-ray maximum because the 6 cm observations are most sensitive to the highest energy electrons ($\gtrsim 100$ keV electron energies) produced in the flare, and more of these electrons are present at 1553 UT.

The evolution of the X-ray emission can be seen more clearly from spectral fits to the HXRBS data. The X-ray data throughout the period of the flare was found to be acceptably fitted by a power-law spectrum. The resulting time profiles for the amplitude coefficient (A_1) and the spectral index (A_2) are shown in Figures 4*a* and *b* for a spectral fit of the form $I(E) = A_1(E/50)^{-A_2}$, where $I(E)$ is the X-ray flux in photons cm^{-2} s^{-1} keV^{-1} at photon energy E, in keV. The general trend is for the spectrum to soften (steepen) as the flare progresses. The spectrum hardens (flattens) significantly, however, at $15^h53^m.4$ UT, where the 6 cm emission is maximum, and in a double peak at $15^h51^m.7$ UT, as reflected in the 56–129 and 104–498 keV light curves (Fig. 2). (The double peak at $15^h51^m.7$ UT shows up clearly in the 8.8 GHz light curve.) There is also some hardening of the spectrum at 15^h52^m UT, where the integrated X-ray emission is greatest. The spectrum consistently hardens where there are peaks in the intensity, indicating that higher energy electrons are produced at these times.

We have computed the power flux of electrons with $E > 25$ keV throughout the flare, assuming that the X-ray emission is thick-target bremsstrahlung. The results are shown

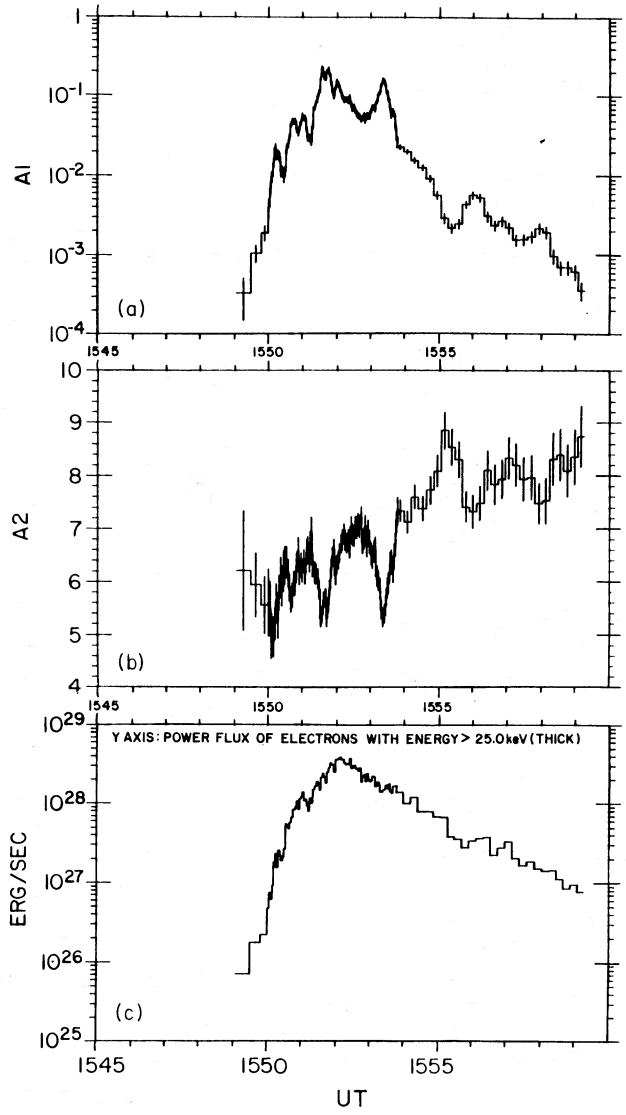

FIG. 4.—(*a*), (*b*): Time profiles of the HXRBS X-ray amplitude coefficient (A_1) and spectral index (A_2) are shown for a spectral fit of the form $I(E) = A_1(E/50)^{-A_2}$, where $I(E)$ is the X-ray flux in photons cm^{-2} s^{-1} keV^{-1} at photon energy E, in keV. (*c*): The time profile of the power flux of $E > 25$ keV electrons is shown, as derived from the HXRBS X-ray data. The X-ray emission is assumed to be thick-target bremsstrahlung.

in Figure 4*c*. The total flare energy in electrons with $E > 25$ keV (assuming thick-target bremsstrahlung) is 10^{31} ergs. Of note is the relative smoothness of the curve (cf. Figs. 2, 4*a*, and 4*b*). In particular, there is no significant change in the downward trend of the power flux at $15^h53^m.4$ UT, when the 6 cm emission is greatest and the X-ray spectrum hardens. Hence, although the largest number of electrons with $E > 100$ keV is produced at this time, there is no significant increase in the total power flux of electrons with $E > 25$ keV. This can be understood as follows: for an electron energy spectrum of the form $N(\epsilon) = K(\epsilon/\epsilon_{min})^{-\gamma}$, the power flux of electrons with $\epsilon > \epsilon_{min}$ is $K\epsilon_{min}^2/(\gamma - 2)$. Since K is the number of electrons at ϵ_{min}, the power flux is sensitive to the number of low-energy electrons ($\epsilon \approx \epsilon_{min}$), but not very sensitive to

changes in the number of high-energy electrons. For a hardening of the electron spectrum from $\gamma = 7$ to $\gamma = 5$ with no change in K, for example, the power flux increases by a factor of 1.67. The absence of an increase in the electron power flux at 1553.4 UT indicates that either a new population of electrons with a flatter spectrum and few 25 keV electrons has been produced at this time, and coexists with the old, steeper spectrum population of electrons (this possibility is not ruled out by the HXRBS spectral data), or all of the particles are part of a single population of electrons and K has decreased. Taking all of the particles with $E > 25$ keV to be part of a single population of electrons (the entire spectrum is acceptably represented by a single power law), this implies that in the secondary peaks such as that at 1553 UT, already energetic electrons ($E \gtrsim 25$ keV) are accelerated up to higher energies so that the total energy in particles with $E \gtrsim 25$ keV is approximately conserved. (If particles with energies less than 25 keV were uniformly accelerated into the $E > 25$ keV energy range, K would not decrease and the electron power flux would increase.) Therefore, it follows that, if only a single population of electrons is involved, the primary process in these peaks is not the acceleration of a less energetic population of electrons up into the $E \gtrsim 25$ keV energy range. On the other hand, the general rise and fall reflected in Figure 4*c* does represent the acceleration of lower energy particles into this energy range, with fewer of the highest energy electrons being produced later in the flare (reflected in the trend toward a softer spectrum in Fig. 4*b*).

Microwave spectra, derived from the Sagamore Hill light curves in Figure 3, are shown for several times during the flare in Figure 5. The solid curves are interpolations between the four data points and, hence, should not be taken too seriously. The spectra indicate that the 6 cm emission is optically thick throughout the flare, confirming the conclusion of KSV based upon comparison of the 6 cm polarization data with magnetograms (the 6 cm polarization is deduced to be ordinary mode). The data indicate that the microwave spectra peak at a frequency just above 5 GHz, and this peak does not vary by more than a few GHz throughout the flare. The spectra tend to flatten (on both sides of the peak) as the flare progresses. The low-frequency spectral index, defined by $\alpha_L = \ln (F_5/F_{2.7})/\ln (5/2.7)$, where F_5 and $F_{2.7}$ are the 5 GHz and 2.7 GHz radio fluxes, is generally less than 2.0. At $15^h53^m.4$ UT, however, when the 6 cm flux is greatest, α_L increases to a value of 2.25 (with an estimated possible error of ± 0.10). A spectrum this steep is not expected for a self-absorbed thermal source. (A single, isothermal source will give $\alpha_L = 2.0$. A multithermal source can only give a flatter spectrum.) Hence, we conclude that either the emission is nonthermal or the low-frequency turnover in the radio spectrum is due to external absorption rather than self-absorption. If the turnover is not due to self-absorption, however, the ordinary mode polarization deduced for the 6 cm emission would not be explained.

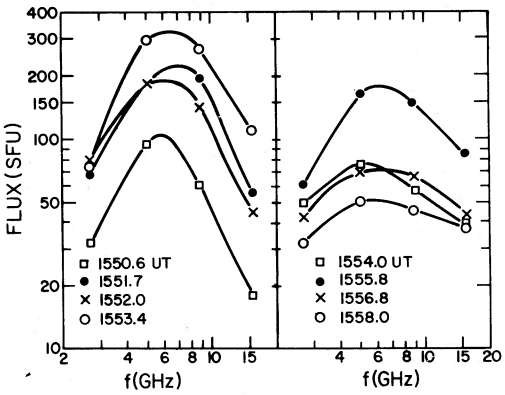

FIG. 5.—Microwave spectra are shown for selected times during the rise and declining phases of the flare. The microwave fluxes (in solar flux units) are obtained from the Sagamore Hill light curves (Fig. 3).

It is interesting that the 2.7 GHz flux reaches its highest value at 15^h52^m UT, the same time as the maximum of the integrated X-ray flux, rather than at $15^h53^m.4$ UT, when the flux is maximum at higher frequencies (see Fig. 3). Since the low-frequency microwave spectrum is much steeper at $15^h53^m.4$ UT than at 15^h52^m UT, the 2.7 GHz flux at 1552 UT exceeds that at 1553.4 UT. The low-frequency spectrum of the secondary peaks at $15^h51^m.7$ UT is also steep enough for the 2.7 GHz flux at 1552 UT to exceed that at 1551.7 UT. Hence, the time profile of the 2.7 GHz flux more closely resembles the integrated X-ray light curve than that of the flux at the higher microwave frequencies. The higher frequency (optically thin) 8.7 and 15.4 GHz light curves, on the other hand, more closely resemble the 104–498 keV X-ray light curve.

Because of the small number of data points and their closeness to the peak of the microwave spectrum, a meaningful quantitative comparison of the high-frequency microwave spectral index with the X-ray spectral index at a given time in the flare is not possible. The magnitude of the high-frequency spectral index is most likely equal to or greater than that which can be determined from the 8.7 and 15.4 GHz fluxes [$\alpha_H = \ln (F_{15.4}/F_{8.8})/\ln (15.4/8.8)$]. The electron energy spectrum implied by the X-ray spectrum is generally steeper than that which is deduced from α_H. This discrepancy becomes greater in the later stages of the flare. When the 6 cm radio flux is maximum (1553.4 UT), $\alpha_H \approx 1.6$. Taking the synchrotron theory for fully relativistic electrons to be approximately valid, this implies an electron energy index of $\gamma \approx 4.2$ [$N(\epsilon) \propto \epsilon^{-\gamma}$, where $N(\epsilon)$ the number of electrons keV^{-1} and ϵ is the electron energy]. This is close to the electron spectrum which is deduced from the X-ray spectrum ($A_2 \approx 5$; see Fig. 4*b*) if the X-ray emission is thin-target bremsstrahlung (see Brown 1971). The microwave and hard X-ray spectra at 1551.7 UT are most easily understood, however, if the X-ray emission is thick-target bremsstrahlung. The available data clearly do not lead to a simple model with the microwave and hard X-ray emissions arising from a single ensemble of electrons. The general flattening of the radio spectrum as the flare progresses (as opposed to the softening trend in the X-ray spectrum), most likely reflects the decline in the dominence of a single-source region (A), with emission from several regions (with somewhat different physical conditions) contributing to the radio spectrum, broadening the spectral peak.

IV. DISCUSSION AND CONCLUSIONS

We have found that the individual bipolar sources observed with the VLA vary together, rather than sequentially or in

an uncorrelated manner. This indicates that, if the multiple arcade structure indicated by the cleaned VLA maps is real, the arcades must all be excited by a common driver, or the instability in one of the arcades must be transmitted to the nearby structures within the 10 s time resolution of the VLA observations. This requires a signal speed of 1700 km s^{-1} or greater. Other than a possible increase in the altitude of the flaring arcades (discussed by KSV), the 2″ angular resolution VLA maps indicate no significant change in the magnetic field structure throughout the observed period of the flare (1550.8–1559.6 UT).

The 6 cm flux maximum is found not to coincide with the 28–498 keV X-ray flux maximum because the X-ray spectrum (and, hence, the electron energy spectrum) is relatively soft when the X-ray maximum occurs. The long-term trend throughout the flare is for the X-ray spectrum to steepen as the flare progresses. The X-ray spectrum consistently hardens in the secondary peaks, however. This behavior of the spectral index is not consistent with betatron acceleration and deceleration of the electrons, which can occur in a magnetic trap as the flaring loop (or loops) contracts and expands (Brown and Hoyng 1975; Brown and McClymont 1976; Karpen 1982). The betatron acceleration model of Brown and Hoyng predicts that the X-ray spectrum should steepen when the flux increases; contrary to the observed behavior. The hardening of the spectrum in the peaks is consistent with Fermi acceleration models, such as that of Benz (1977), however.

The steep, low-frequency radio spectrum ($\alpha_L = 2.25$) when the 6 cm emission is maximum indicates that the emission at this time is nonthermal. Although a multithermal source may produce a spectrum flatter than $\alpha_L = 2.0$, a steeper spectrum cannot be obtained. An alternative possibility is that the microwave emission is not self-absorbed, and the spectral turnover is caused by an external absorption process. This is less likely, however, since the ordinary mode polarization deduced from the 6 cm VLA maps is most easily explained as optically thick, nonthermal emission. The extended structure of the individual 6 cm sources is also most easily understood in terms of self-absorbed emission. The microwave loop models of Petrosian (1981) have shown that optically thick emission from isotropic electrons will produce an extended source in the upper part of the loop (see also Holman, Kundu, and Papadopoulos 1982), as was observed at 6 cm by KSV. If the emission is not self-absorbed, a more compact source is expected. Hence, the microwave and hard X-ray spectra and the spatial structure of the 6 cm sources are most easily understood in terms of emission from a nonthermal distribution of electrons which is optically thick at 6 cm and longer wavelengths.

The power flux of electrons with $E \geq 25$ keV (Fig. 4) is found not to increase significantly at the time of the 6 cm maximum. The hard X-ray spectrum flattens from $A_2 \approx 7$ to $A_2 \approx 5$ (Fig. 3), however. If a single, power-law distribution of electrons is contributing to the X-ray emission, the absence of an increase in the electron power flux indicates that the already energetic, $E \geq 25$ keV electrons with $A_2 \approx 7$ are accelerated until $A_2 \approx 5$, but no additional particles are accelerated into the $E \geq 25$ keV energy range. Hence, either two acceleration mechanisms are required, or the acceleration mechanism must only operate on higher energy particles later in the flare, when the spectrally hard secondary peak occurs. Alternatively, a new population of electrons with a flatter spectrum and fewer 25 keV particles may have been accelerated into the $E > 25$ keV energy range. These particles must have simultaneously been emitting X-rays with the preexisting, steeper spectrum population of electrons, ruling out a simple, thick-target beam model with a single acceleration region for the total hard X-ray emission.

The authors thank R. A. Shine for his invaluable assistance in producing the 6 cm light curves, and E. W. Cliver for supplying the Sagamore Hill light curves. The 6 cm light curves were obtained using the SMM/UVSP PDP-11 computer at NASA Goddard Space Flight Center. We thank the referee for some comments which led to a clarification of the conclusions of this paper. This work was supported in part by NASA grant NGR 21-002-199, NASA contract NSG 5320, and NSF grant ATM 81-03809.

REFERENCES

Benz, A. O. 1977, *Ap. J.*, **211**, 270.
Brown, J. C. 1971, *Solar Phys.*, **18**, 489.
Brown, J. C., and Hoyng, P. 1975, *Ap. J.*, **200**, 734.
Brown, J. C., and McClymont, A. H. 1976, *Solar Phys.*, **49**, 329.
Holman, G. D., Kundu, M. R., and Papadopoulos, K. 1982, *Ap. J.*, **257**, 354.
Karpen, J. T. 1982, *Solar Phys.*, **77**, 205.
Kundu, M. R., Schmahl, E. J., and Velusamy, T. 1982, *Ap. J.*, **253**, 963.
Orwig, L. E., Frost, K. J., and Dennis, B. R. 1980, *Solar Phys.*, **65**, 25.
Petrosian, V. 1982, *Ap. J. (Letters)*, **255**, L85.

B. R. Dennis: Code 602.6, Laboratory for Astronomy and Solar Physics, NASA Goddard Space Flight Center, Greenbelt, MD 20771

Gordon D. Holman and M. R. Kundu: Astronomy Program, University of Maryland, College Park, MD 20742